DYNAMICAL ELECTROWEAK SYMMETRY BREAKING: IMPLICATIONS OF THE H

Written October 2013 by R.S. Chivukula (Michigan State University), M. Narain (Brown University), and J. Womersley (STFC, Rutherford Appleton Laboratory).

1. Introduction and Phenomenology

In theories of dynamical electroweak symmetry breaking, the electroweak interactions are broken to electromagnetism by the vacuum expectation value of a composite operator, typically a fermion bilinear. In these theories, the longitudinal components of the massive weak bosons are identified with composite Nambu-Goldstone bosons arising from dynamical symmetry breaking in a strongly-coupled extension of the standard model. Viable theories of dynamical electroweak symmetry breaking must also explain (or at least accommodate) the presence of an additional composite scalar state to be identified with the H scalar boson [1,2] – a state unlike any other observed to date.

Theories of dynamical electroweak symmetry breaking can be classified by the nature of the composite singlet state to be associated with the H, and the corresponding dimensional scales f, the analog of the pion decay-constant in QCD, and Λ, the scale of the underlying strong dynamics.[1] Of particular importance is the ratio v/f, where $v^2 = 1/(\sqrt{2}G_F) \approx (246\,\mathrm{GeV})^2$, since this ratio measures the expected size of the deviations of the couplings of a composite Higgs boson from those expected in the standard model. The basic possibilities, and the additional states that they predict, are described below.

1.1 Technicolor, $v/f \simeq 1$, $\Lambda \simeq 1$ TeV:

Technicolor models [8–10] incorporate a new asymptotically free gauge theory ("technnicolor") and additional massless fermions ("technifermions" transforming under a vectorial representation of the gauge group). The global chiral symmetry of the fermions is spontaneously broken by the formation of a

[1] In a strongly interacting theory "Naive Dimensional Analysis" [3,4] implies that, in the absence of fine-tuning, $\Lambda \simeq g^* f$ where $g^* \simeq 4\pi$ is the typical size of a strong coupling in the low-energy theory [5,6]. This estimate is modified in the presence of multiple flavors or colors [7].

technifermion condensate, just as the approximate chiral symmetry in QCD is broken down to isospin by the formation of a quark condensate. The $SU(2)_W \times U(1)_Y$ interactions are embedded in the global technifermion chiral symmetries in such a way that the only unbroken gauge symmetry after chiral symmetry breaking is $U(1)_{em}$.[2] These theories naturally provide the Nambu-Goldstone bosons "eaten" by the W and Z boson, and there are various possibilities for the scalar H as described below.

In these theories there would typically be additional states (e.g. vector mesons, analogous to the ρ and ω mesons in QCD) with TeV masses [14,15], and the WW and ZZ scattering amplitudes would expected to be strong at energies of order 1 TeV. In all of these cases, however, to the extent that the H has couplings consistent with those of the standard model, these theories are very highly constrained.

a) **H as a singlet scalar resonance:** The strongly-interacting fermions which make up the Nambu-Goldstone bosons eaten by the weak bosons would naturally be expected to also form an isoscalar neutral bound state, analogous to the σ particle expected in pion-scattering in QCD [16]. However, in this case, there is no symmetry protecting the mass of such a particle – which would therefore generically be of order the energy scale of the underlying strong dynamics Λ. In the simplest theories of this kind – those with a global $SU(2)_L \times SU(2)_R$ chiral symmetry which is spontaneously broken to $SU(2)_V$ – the natural dynamical scale Λ would be of order a TeV, resulting in a particle too heavy to be identified with the H. The scale of the underlying interactions could naturally be smaller than 1 TeV if the global symmetries of the theory are larger than $SU(2)_L \times SU(2)_R$, but in this case there would be additional (pseudo-)Nambu-Goldstone bosons (more on this below). A theory of this kind would only be viable, therefore, if some choice of the parameters of the high energy theory could give rise to sufficiently light state without the appearance of additional particles that should have already been observed. Furthermore, while a

[2] For a review of technicolor models, see [11–13].

particle with these quantum numbers could have Higgs-like couplings to any electrically neutral spin-zero state made of quarks, leptons, or gauge-bosons, there is no symmetry insuring that the coupling strengths of such a composite singlet scalar state would be precisely the same as those of the standard model Higgs.

b) **H as a dilaton:** It is possible that the underlying strong dynamics is approximately scale-invariant, as inspired by theories of "walking technicolor" [17–21], and that both the scale and electroweak symmetries are spontaneously broken at the TeV energy scale [22]. In this case, due to the spontaneous breaking of approximate scale invariance, one might expect a corresponding (pseudo-) Nambu-Goldstone boson with a mass less than a TeV, the dilaton.[3] A dilaton couples to the trace of the energy momentum tensor, which leads to a simllar pattern of two-body couplings as the couplings of the standard model Higgs boson [27–29]. Scale-invariance is a space-time symmetry, however, and by the Coleman-Mandula theorem [30], we know that space-time symmetries cannot be embedded in a larger symmetry which includes the global symmetries that we can identify with the electroweak group. Therefore the decay-constants associated with the breaking of the scale and electroweak symmetries will not, in general, be precisely the same.[4] In other words, if there are no large anomalous dimensions associated with the W- and Z-bosons or the top- or bottom-quarks, the ratios of the couplings of the dilaton to these particles would be the same as the ratios of the same couplings for the standard model Higgs boson, but the overall strength of the dilaton couplings would be expected to be different [31,32]. Furthermore, the couplings of the dilaton to gluon- and photon-pairs can be related to the

[3] Even in this case, however, a dilaton associated with electroweak symmetry breaking will likely not *generically* be as light as the H [23–26].

[4] If both the electroweak symmetry and the approximate scale symmetry are broken only by electroweak doublet condensate(s), then the decay-constants for scale and electroweak symmetry breaking may be approximately equal – differing only by terms formally proportional to the amount of explicit scale-symmetry breaking.

beta functions of the corresponding gauge interactions in the underlying high-energy theory, and will not in general yield couplings with the exactly the same strengths as the standard model.

c) **H as a singlet Pseudo-Nambu-Goldstone Boson:** If the global symmetries of the technicolor theory are larger than $SU(2)_L \times SU(2)_R$, there can be extra singlet (pseudo-) Nambu-Goldstone bosons which could be identified with the H. In this case, however, the coupling strength of the singlet state to WW and ZZ pairs would be comparable to the couplings to gluon and photon pairs, and these would all arise from loop-level couplings in the underlying technicolor theory [33]. This pattern of couplings is not supported by the data.

1.2 The Higgs doublet as a pseudo-Nambu-Goldstone Boson, $v/f < 1$, $\Lambda > 1$ TeV:

In technicolor models, the symmetry-breaking properties of the underlying strong dynamics necessarily breaks the electroweak gauge symmetries. An alternative possibility is that the underlying strong dynamics itself does not break the electroweak interactions, and that the entire quartet of bosons in the Higgs doublet (including the state associated with the H) are composite (pseudo-) Nambu-Goldstone particles [34–37]. In this case, the underlying dynamics can occur at energies larger than 1 TeV and additional interactions with the top-quark mass generating sector (and possibly with additional weakly-coupled gauge bosons) cause the vacuum energy to be minimized when the composite Higgs doublet gains a vacuum expectation value [38]. In these theories, the couplings of the remaining singlet scalar state would naturally be equal to that of the standard model Higgs boson up to corrections of order $(v/f)^2$ and, therefore, constraints on the size of deviations of the H couplings from that of the standard model Higgs give rise to lower bounds on the scales f and Λ.

The electroweak gauge interactions, as well as the interactions responsible for the top-quark mass, explicitly break the chiral symmetries of the composite Higgs model, and lead generically to sizable corrections to the mass-squared of the

Higgs-doublet – the so-called "Little Hierarchy Problem" [39]. "Little Higgs" theories [40–43] are examples of composite Higgs models in which the (collective) symmetry-breaking structure is selected so as to suppress these contributions to the Higgs mass-squared, while allowing for a sufficiently large Higgs-boson self-coupling. The collective symmetry breaking required in Little Higgs models typically requires a larger global symmetry of the underlying theory, and hence additional relatively light (compared to Λ) scalar particles, extra electroweak vector bosons (e.g. an additional $SU(2) \times U(1)$ gauge group), and vector-like partners of the top-quark of charge $+2/3$ and possibly also $+5/3$ [44]. Finally, in addition to these states, one would expect the underlying dynamics to yield additional scalar and vector resonances with masses of order Λ.

1.3 Top-Condensate, Top-Color, Top-Seesaw and related theories, $v/f < 1$, $\Lambda > 1$ TeV:

A final alternative is to consider a strongly interacting theory with a high (compared to a TeV) underlying dynamical scale that *would* naturally break the electroweak interactions, but whose strength is adjusted ("fine-tuned") to produce electroweak symmetry breaking at 1 TeV. This alternative is possible if the electroweak (quantum) phase transition is continuous (second order) in the strength of the strong dynamics [45]. If the fine tuning can be achieved, the underlying strong interactions will produce a light composite Higgs bound state with couplings equal to that of the standard model Higgs boson up to corrections of order $(1\ \mathrm{TeV}/\Lambda)^2$. As in theories in which electroweak symmetry breaking occurs through vacuum alignment, therefore, constraints on the size of deviations of the H couplings from that of the standard model Higgs give rise to lower bounds on the scale Λ. Formally, in the limit $\Lambda \to \infty$ (a limit which requires arbitrarily fine adjustment of the strength of the high-energy interactions), these theories are equivalent to a theory with a fundamental Higgs boson – and the fine adjustment of the coupling strength is a manifestation of the hierarchy problem of theories with a fundamental scalar particle.

In many of these theories the top-quark itself interacts strongly (at high energies), potentially through an extended

color gauge sector [46–49]. In these theories, top-quark condensation (or the condensation of an admixture of the top with additional vector-like quarks) is responsible for electroweak symmetry breaking, and the H is identified with a bound state involving the third generation of quarks. These theories typically include an extra set of massive color-octet vector bosons (top-gluons), and an extra $U(1)$ interaction (giving rise to a top-color Z') which couple preferentially to the third generation and whose masses define the scale Λ of the underlying physics.

In addition to the electroweak symmetry breaking dynamics described above, which gives rise to the masses of the W and Z particles, additional interactions must be introduced to produce the masses of the standard model fermions. Two general avenues have been suggested for these new interactions. In one case, e.g. "extended technicolor" theories [50,51], the gauge interactions in the underlying strongly interacting theory are extended to incorporate flavor. This extended gauge symmetry is broken down (possibly sequentially, at several different mass scales) to the residual strongly-interacting interaction responsible for electroweak symmetry breaking. The massive gauge-bosons corresponding to the broken symmetries then mediate interactions between mass operators for the quarks/leptons and the corresponding bilinears of the strongly-interacting fermions, giving rise to the masses of the ordinary fermions after electroweak symmetry breaking. An alternative proposal, "partial compositeness" [52], postulates additional interactions giving rise to mixing between the ordinary quarks and leptons and massive composite fermions in the strongly-interacting underlying theory. Theories incorporating partial compositeness include additional vector-like partners of the ordinary quarks and leptons, typically with masses of order a TeV or less.

In both cases, the effects of these flavor interactions on the electroweak properties of the ordinary quarks and leptons are likely to be most pronounced in the third generation of fermions.[5] The additional particles present, especially the addi-

[5] Indeed, from this point of view, the vector-like partners of the top-quark in top-seesaw and little Higgs models can be viewed as incorporating partial compositeness to explain the origin of the top quark's large mass.

tional scalars, often couple more strongly to heavier fermions. Moreover, since the flavor interactions must give rise to quark mixing, we expect that a generic theory of this kind could give rise to large flavor-changing neutral-currents [51] – though these constraints are typically somewhat relaxed if the theory "walks" [17–21] or if $\Lambda > 1$ TeV [53]. For these reasons, most authors assume that the underlying flavor dynamics respects flavor symmetries ("minimal" [54,55] or "next-to-minimal" [56] flavor violation) which suppress flavor-changing neutral currents in the two light generations.[6] Additional considerations apply when extending these considerations to potential explanation of neutrino masses (see, for example, [59,60]) .

Since the underlying high-energy dynamics in these theories are strongly coupled, there are no reliable calculation techniques that can be applied to analyze their properties. Instead, most phenomenological studies depend on the construction of a "low-energy" effective theory describing additional scalar, fermion, or vector boson degrees of freedom, which incorporates the relevant symmetries and, when available, dynamical principles. In some cases, motivated by the AdS/CFT correspondence [61], the strongly-interacting theories described above have been investigated by analyzing a dual compactified five-dimensional gauge theory. In these cases, the AdS/CFT "dictionary" is used to map the features of the underlying strongly coupled high-energy dynamics onto the low-energy weakly coupled dual theory [62].

More recently, progress has been made in investigating strongly-coupled models using lattice gauge theory [63,64]. These calculations offer the prospect of establishing which strongly coupled theories of electroweak symmetry breaking have a particle with properties consistent with those observed for the H – and for establishing concrete predictions for these theories at the LHC [65].

[6] In theories of partial compositeness, the masses of the ordinary fermions depend on the scaling-dimension of the operators corresponding to the composite fermions with which they mix. This leads to a new mechanism for generating the mass-hierarchy of the observed quarks and leptons that, potentially, incorporates minimal or next-to-minimal flavor violation [57,58].

2. Experimental Searches

As discussed above, the extent to which the couplings of the H conform to the expectations for a standard model Higgs boson constrains the viability of each of these models. Measurements of the H couplings, and their interpretation in terms of effective field theory, are summarized in the H review in this volume. In what follows, we will focus on searches for the additional particles that might be expected to accompany the singlet scalar: extra scalars, fermions, and vector bosons. In some cases, detailed model-specific searches have been made for the particles described above (though generally not yet taking account of the demonstrated existence of the H boson).

In most cases, however, generic searches (e.g. for extra W' or Z' particles, extra scalars in the context of multi-Higgs models, or for fourth-generation quarks) are quoted that can be used – when appropriately translated – to derive bounds on a specific model of interest.

The mass scale of the new particles implied by the interpretations of the low mass of H discussed above, and existing studies from the Tevatron and lower-energy colliders, suggests that only the Large Hadron Collider has any real sensitivity. A number of analyses already carried out by ATLAS and CMS use relevant final states and might have been expected to observe a deviation from standard model expectations – in no case so far has any such deviation been reported. The detailed implications of these searches in various model frameworks are described below.

2.1 W' or Z' Bosons

Massive vector bosons or particles with similar decay channels would be expected to arise in Little Higgs theories, in theories of Technicolor, or models involving a dilaton, adjusted to produce a light Higgs boson, consistent with the observed H. These particles would be expected to decay to pairs of vector bosons, to third generation quarks, or to leptons. The generic searches for W' and Z' vector bosons listed below can, therefore, be used to constrain models incorporating a composite Higgs-like boson. ATLAS [74] and CMS [75] have searched for Z' production with $Z' \to ee$ or $\mu\mu$ in collision data recorded at

$\sqrt{s} = 8$ TeV during the 2012 run of the LHC. These searches are carried out using a integrated luminosity of 20 fb^{-1} and 20.6 fb^{-1} by ATLAS and CMS respectively. The main backgrounds to these analyses arise from Drell-Yan, $t\bar{t}$, and diboson production and are estimated using Monte Carlo, with the cross sections scaled by next-to-next-to-leading-order k-factors. Instrumental backgrounds from QCD multijet and W+jet events are estimated using control data samples. One of the challenges of this analysis is the modeling of the dilepton pair invariant mass resolution. The dielectron channel has higher sensitivity due to the superior mass resolution compared to the dimuon channel. No deviation from the standard model prediction is seen in the dielectron and dimuon invariant mass spectra, by either the ATLAS or the CMS analysis, and lower limits on possible Z' boson masses are set. A $Z'_{\rm SSM}$ with couplings equal to the standard model Z (a "sequential standard model" Z') and a mass below 2.86 TeV is excluded by ATLAS, while CMS sets a 95% C.L. lower mass limit of 2.96 TeV. The ATLAS analysis rules out various $E6$-motivated bosons (Z'_{ψ}, Z'_{χ}) with masses lower than $2.38 - 2.54$ TeV. A Z'_{ψ} with a mass below 2.6 TeV is excluded by CMS. ATLAS searches are also interpreted to obtain a lower mass limit of 2.47 TeV for a Randall-Sundrum graviton with coupling parameter $k/\overline{M}_{Pl} = 0.1$. In addition, ATLAS has performed a search for Z' decaying to a ditau final state [76]. An excess in this signature could have interesting implications for models in which lepton universality is not a necessary requirement and enhanced couplings to the third generation are allowed. This analysis leads to a lower limit on the mass of $Z'_{\rm SSM}$ of 1.9 TeV.

ATLAS [77] has also searched for Z' bosons decaying into top quark pairs using 14 fb^{-1} of collision data collected at $\sqrt{s} = 8$ TeV. The lepton plus jets final state is used, where the top quark pair decays as $t\bar{t} \rightarrow WbWb$ with one W boson decaying leptonically and the other hadronically. CMS [70] has carried out a similar search for Z' resonances decaying to $t\bar{t}$ pairs, using "semi-leptonic" and "all-hadronic" decays of the top quarks. The data sample analyzed corresponds to an integrated luminosity of 19.7 fb^{-1}. Both analyses consider $t\bar{t}$ events at

the kinematic production threshold, and those produced with high Lorentz boosts. In addition to a conventional resolved-jet analysis, large radius jet-substructure identification techniques are used to reconstruct the $t\bar{t}$ resonance. The $t\bar{t}$ invariant mass spectrum is analyzed for any local excess, and no evidence for any resonance is seen.

Upper limits are set by ATLAS on the cross section times branching ratio of a narrow Z' boson decaying to top quark pairs ranging from 5.3 pb for a Z' mass of 0.5 TeV to 0.08 pb for a mass of 3 TeV. A narrow leptophobic topcolor Z' boson, with $\Gamma/m = 1.2\%$, and a mass below 1.8 TeV is excluded, and upper limits are also set on the cross section times branching ratio for a broad Kaluza Klein excitation of the gluon (g_{KK}) with $\Gamma/m = 15.3\%$ decaying to $t\bar{t}$ which range from 9.6 pb for a mass of 0.5 TeV to 0.152 pb for a mass of 2.5 TeV.

CMS sets upper limits on the production cross section times branching ratio for narrow (wide) resonances at 1.94(1.71) pb for a mass of 0.5 TeV, and 0.029(0.045) pb for a mass of 2 TeV. Topcolor Z' bosons with masses below 2.1 TeV and 2.7 TeV are excluded for $\Gamma/m = 1.2\%$ and 10%, respectively. In the Randall-Sundrum model, g_{KK} masses below 2.5 TeV are excluded.

The semi-leptonic analysis is sensitive to a spin-zero resonance with narrow width, produced via gluon fusion without interference with the standard model background. For heavy Higgs-like particles decaying into $t\bar{t}$, CMS obtains upper limits on the cross sections of 0.8 pb and 0.3 pb for spin-zero resonances with masses of 500 and 750 GeV, respectively [70].

CMS [94] has additionally searched for heavy Z' resonances decaying to the $b\bar{b}$ final state by selecting event with dijets with one or both of the jets tagged as a b-jet. The search is performed using 19.6 fb^{-1} of data collected at $\sqrt{s}$=8 TeV and excludes a sequential standard model Z' with a mass between 1.20 and 1.68 TeV, when the decay branching ratio of $Z' \to b\bar{b}$ relative to $Z' \to jj$ is taken to be 0.22.

Both ATLAS and CMS have also searched for massive charged vector bosons. ATLAS [88] and CMS [89] have searched for a resonant W' state decaying to WZ in the fully-leptonic

channel, $\ell\nu\ell'\ell'$ (where $\ell, \ell' = e, \mu$). The WZ invariant mass distribution reconstructed from the observed lepton and neutrino momenta and L_T, the scalar sum of the charged lepton p_Ts, are used as the discriminating variables to identify the W' signal and reject the backgrounds. The backgrounds are mainly from standard model WZ production. No significant localized excess is observed in the reconstructed WZ invariant mass distribution. Using a sample of 19.6 fb^{-1} of data recorded at $\sqrt{s} = 8$ TeV, CMS excludes a W' with masses between 0.17 and 1.45 TeV. The analysis by ATLAS, based on 13 fb^{-1} collected at $\sqrt{s} = 8$ TeV, derives upper limits on the production cross section times branching ratio and obtains a bound on the W' mass of 1.18 TeV in the context of benchmark Extended Gauge models.

CMS [90] also performed a search for $W' \to WZ$ using dijet events, with one or both of the jets identified as a W or a Z boson using jet-substructure techniques. In the absence of any excess, a W' decaying into WZ is excluded up to 1.73 TeV at 95% C.L.

Searches by CMS [91] for a heavy W' decaying to $e\nu$ or $\mu\nu$ again yield a null signal, allowing a standard model-like W' with masses up to 3.35 TeV to be excluded. This result can be re-interpreted to rule out a split UED Kaluza-Klein W^2_{KK} excitation below 3.7 TeV for the mass parameter μ=10 TeV, and in addition set a limit on the scale of a new helicity non-conserving four-fermion contact interaction Λ of 13.0 (10.9) TeV for the electron (muon) channel.

Heavy new gauge bosons can couple to left-handed fermions like the W boson or to right-handed fermions. W' bosons that couple only to right-handed fermions may not have leptonic decay modes, depending on the mass of the right-handed neutrino. For these W' bosons, the tb decay mode is especially important because it is the hadronic decay mode with the best signal-to-background. CMS [92] has carried out a search for $W' \to tb$ decays followed by $t \to bW$ and $W \to \ell\nu$. The analysis relies on the invariant mass of the W', using $\ell\nu$+jets events with one or more b-tags and uses multivariate techniques to improve signal to background separation. The measurement is carried

out for arbitrary combinations of the coupling strengths of the W' to left- and right-handed fermions. Based on an analysis of 19.6 fb^{-1} of data, W' bosons with purely left-handed (right-handed) couplings to fermions are excluded for masses below 2.09 (2.03) TeV. ATLAS [93] has also searched for W' bosons in single-top quark production, using 14.3 fb^{-1} of data recorded at $\sqrt{s} = 8$ TeV. The analysis looks at the $\ell\nu b\overline{b}$ final state ($\ell = e, \mu$) again using a multivariate method. No significant deviation from the standard model expectation is observed and for a left-handed (right-handed) W' boson, masses below 1.74 (1.84) TeV are excluded at the 95% confidence level.

2.2 Technicolor Resonances

While the W' and Z' searches listed above have not been interpreted in terms of specific technicolor models, the technicolor-inspired searches listed here have been carried out at the LHC.

ATLAS has searched for a dijet resonance [86] with an invariant mass in the range $130 - 300$ GeV, produced in association with a W or a Z boson. The analysis used 20.3 fb^{-1} of data recorded at $\sqrt{s} = 8$ TeV. The W or Z boson is required to decay leptonically ($\ell = e, \mu$). No significant deviation from the standard model prediction is observed and limits are set on the production cross section times branching ratio for a hypothetical technipion produced in association with a W or Z boson from the decay of a technirho particle in the context of Low Scale Technicolor models.

Both ATLAS and CMS searches for a resonant W' state decaying to WZ in the fully-leptonic channel, $\ell\nu\ell'\ell'(\ell, \ell' = e, \mu)$, described earlier [88,89], have also been used to place limits on a technirho decaying to WZ in similar models.

2.3 Vector-like third generation quarks

Vector-like quarks have non-chiral couplings to W bosons, i.e. their left- and right-handed components couple in the same way. They therefore have vectorial couplings to W bosons. Vector-like quarks arise in Little Higgs theories and theories of a composite Higgs with partial compositeness. In the following the notation T quark refers to a vector-like quark with charge 2/3 and the notation B quark refers to a vector-like quark with

charge $-1/3$. T quarks can decay to bW, tZ, or tH. Weak isospin singlets are expected to decay to all three final states with branching fractions of 50%, 25%, 25%, respectively. Weak isospin doublets are expected to decay exclusively to tZ and to tH [67]. Analogously, B quarks can decay to tW, bZ, or bH. All limits in this section are quoted at a confidence level of 95%.

Searches for T quarks that decay to W bosons

CMS has searched for pair production of heavy T quarks that decay exclusively to bW [71] based on the data collected at $\sqrt{s} = 7$ TeV in 2011 with an integrated luminosity of 5 fb^{-1}. The analysis selects events with exactly one charged lepton, assuming that the W boson from the second T quark decays hadronically. Under this hypothesis, a 2C kinematic fit can be performed to reconstruct the mass of the T quark. The two-dimensional distribution of reconstructed mass vs H_T is used to test for the signal. H_T is the scalar sum of the missing p_T and the transverse momenta of the lepton and the leading four jets. No excess over standard model backgrounds is observed. This analysis excludes new quarks that decay 100% to bW for masses below 570 GeV.

A search by ATLAS for the production of a heavy T quark together with its antiparticle, assumes a significant branching ratio for subsequent decay into a W boson and a b quark [78]. The search is based on 14.3 fb^{-1} of data recorded at $\sqrt{s} =$ 8 TeV. It uses the lepton+jets final state with an isolated electron or muon and at least four jets, at least one of which must be tagged as a b-jet. The selection is optimized for T quark masses above about 400 GeV by requiring a high boost of the W decay products. No significant excess of events above standard model expectation is observed. For a chiral fourth generation quark with branching ratio $BR(T \to Wb) = 1$, masses lower than 740 GeV are excluded.

Searches for T and B quarks that decay to Z bosons

CMS has performed a search targeted on T quarks that decay exclusively to tZ based on an integrated luminosity of 1.1 fb^{-1} from pp collisions at $\sqrt{s} = 7$ TeV [68]. Selected events must have three isolated charged leptons, two of which must be consistent with a leptonic Z-boson decay. No significant excess was observed. T quark masses below 485 GeV are excluded.

CMS has also searched for the pair-production of a heavy B quark and its antiparticle, one of which decays to bZ based on 19.6 fb^{-1} of data collected at $\sqrt{s} = 8$ TeV. Events with a Z-boson decay to e^+e^- or $\mu^+\mu^-$ and a jet identified as originating from a b quark are selected. The signal from $B \to bZ$ decays would appear as a local enhancement in the bZ mass distribution. No such enhancement is found and B quarks that decay 100% into bZ are excluded below 700 GeV. This analysis also sets upper limits on the branching fraction for $B \to bZ$ decays of 30-100% in the B quark mass range 450-700 GeV.

A complementary search has been carried out by ATLAS for new heavy quarks decaying into a Z boson and a third generation quark [79]. The analysis targets both a new charge +2/3 quark T, with $T \to Zt$, and a new charge -1/3 quark B, with $B \to bZ$. The search uses 14.3 fb^{-1} of data recorded at $\sqrt{s}$=8 TeV. Selected events contain a high transverse momentum Z boson that decays leptonically, together with two b-jets. No significant excess of events above the standard model expectation is observed, and mass limits are set depending on the assumed branching ratios, see Fig. 1. In a weak-isospin singlet scenario, a T (B) quark with mass lower than 585 (645) GeV is excluded, while for a particular weak-isospin doublet scenario, a T (B) quark with mass lower than 680 (725) GeV is excluded.

Searches for T quarks that decay to H bosons

ATLAS has performed a search for $T\overline{T}$ production with an appreciable T quark branching fraction into tH, followed by $H \to b\overline{b}$. These events are characterized by a large number of jets, many of which are b-jets. Thus the event selection requires one isolated electron or muon and at least six jets, two of which

must be tagged as b-jets. The data are classified according to their b-jet multiplicity and the distribution of H_T, the scalar sum of the lepton and jet p_Ts and the missing p_T, is used to search for the signal. No excess of events is found. Weak isospin doublet T quarks are excluded below 790 GeV and weak isospin singlet T quarks are excluded below 640 GeV. This search is orthogonal to the search for T quarks that decay to bW and the results of the two searches are combined.

Searches for T and B quarks in multiple final states

Pair-production of T or B quarks with their antiparticles can result in events with like-sign leptons, for example if the decay $T \to tH \to bWW^+W^-$ is present, followed by leptonic decays of two same-sign W bosons. ATLAS and CMS have searched for this final state. The CMS search is part of the analysis described in the following paragraph. The ATLAS search [73] requires exactly two leptons, both with the same electric charge, at least two jets of which at least one must be tagged as a b-jet, and missing p_T. ATLAS quotes exclusions of some possible branching fraction combinations depending on the mass of the new quarks. T quarks that are electroweak singlets are excluded below 540 GeV and the sensitivity is largest for T quarks that decay exclusively to tH. B quarks that are electroweak singlets are excluded below 590 GeV and the sensitivity for B quarks is maximal if they exclusively decay to tW. The limits set by all the ATLAS searches are superimposed in Fig. 1 and Fig. 2.

An inclusive search by CMS targeted at heavy T quarks decaying to any combination of bW, tZ, or tH is described in Ref. [80]. This analysis is based on the data collected at $\sqrt{s}$ = 8 TeV in 2012 with an integrated luminosity of 19.5 fb^{-1}. Selected events have at least one isolated charged lepton. Events are categorized according to number and flavour of the leptons, the number of jets, and the presence of hadronic vector boson and top quark decays that are merged into a single jet. The use of jet substructure to identify hadronic decays significantly increases the acceptance for high T quark masses. The analysis of the high-background single lepton channels is based on a multivariate algorithm using Boosted Decision Trees. The

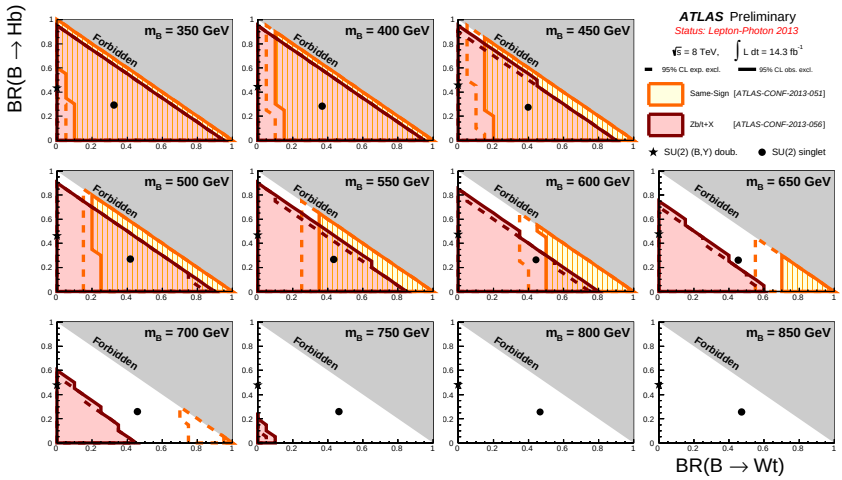

Figure 1: Exclusion limits for BB pair production in the $BR(B \to Wt)$ versus $BR(B \to Ht)$ plane. The limits of the two ATLAS searches are superimposed on the plots. The circle and star symbols denote the default branching ratios for the weak-isospin singlet and doublet cases.

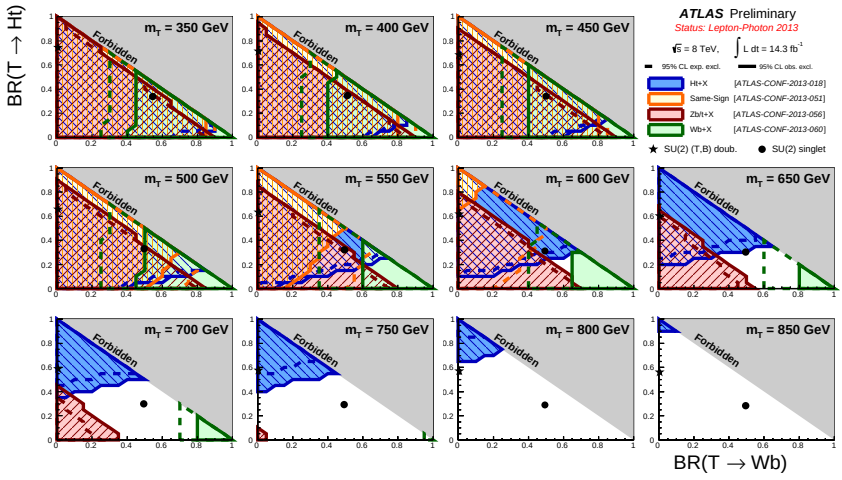

Figure 2: Exclusion limits for TT pair production in the $B(T \to Wb)$ versus $B(T \to Ht)$ plane. The limits of the four ATLAS searches are superimposed on the plots. The circle and star symbols denote the default branching ratios for the weak-isospin singlet and doublet cases.

analysis of the low background multilepton channels is based on the event counts in the individual channels. No excess above standard model backgrounds is observed. Limits on the pair

production cross section of the new quarks are set, combining all event categories, for all combinations of branching fractions into the three final states. For T quarks that exclusively decay to $bW/tZ/tH$, masses below 700/782/706 GeV are excluded. Electroweak singlet vector-like T quarks which decay 50% to bW, 25% to tZ, and 25% to tH are excluded for masses below 696 GeV. The CMS analysis also quotes limits between 690 and 782 GeV on the mass of the T quark for all possible values of the branching fractions into the three different final states bW, tZ and tH. The observed limit for all combination of the three branching fractions is shown in Fig. 3 (left panel). Every point in the triangle corresponds to a particular set of branching fraction values for $T \to bW$, tZ and tH, such that all three add up to one. In Fig. 3 (right panel) the cross section limit is plotted for the nominal combination of branching fractions (50% to bW, 25% to tZ, and 25% to tH).

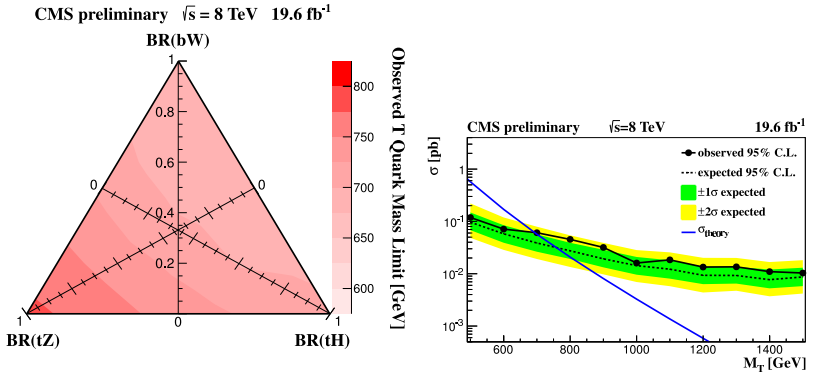

Figure 3: The branching fraction triangle with observed limits for the T quark mass are shown in the left panel. The upper limit on the T quark production cross section for branching fractions into bW, tH, tZ of 50%, 25%, 25% is shown in the right panel [80].

CMS has also carried out a similar inclusive search for the pair production of B quarks that decay into tW, bZ, or bH based on 19.8 fb^{-1} of data collected at $\sqrt{s} = 8$ TeV [81]. Events must have one isolated electron or muon, at least four jets of which at least one is tagged as a b-jet, and missing p_T. Events are classified according to the number of highly boosted

W, Z, or H boson decays. No significant excess of events is observed and B quarks below 582 and 732 GeV are excluded, depending on the B quark decay branching fractions. B quarks that decay exclusively into tW are excluded below 732 GeV. The observed limits for all combinations of branching fractions are shown in Fig. 4, together with the cross section limit plotted for the nominal combination of branching fractions (50% to tW, 25% to bZ, and 25% to bH).

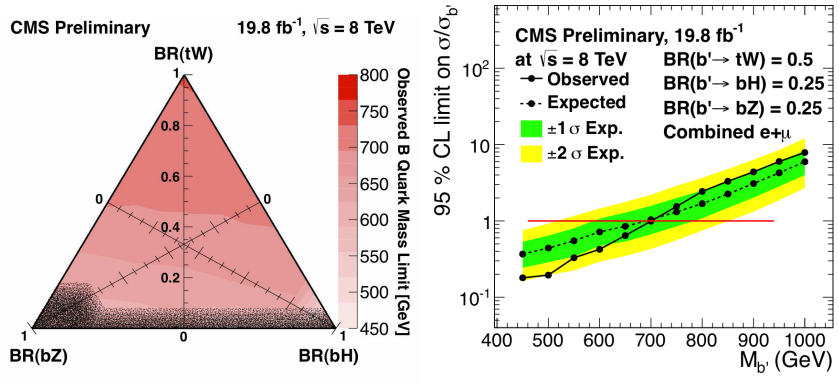

Figure 4: The branching fraction triangle with observed limits for the B quark mass is shown in the left panel. The shaded area at the bottom was not probed by the analysis. The upper limit on the B quark production cross section for branching fractions into mtW, bH, bZ modes of 50%, 25%, 25% respectively, is shown in the right panel [81].

2.4 A charge +5/3 top-partner quark

In models of dynamical electroweak symmetry breaking, the same interactions which give rise to the mass of the top-quark can give unacceptably large corrections to the branching ratio of the Z boson to $b\bar{b}$ [66]. These corrections can be substantially reduced, however, in theories with an extended "custodial symmetry" [44]. This symmetry requires the existence of a charge +5/3 vector-like partner of the top quark.

CMS has performed a search for heavy top with exotic charge 5/3, $T_{5/3}$ vector-like quark following the models in Refs. [82,83]. CMS has searched for the pair-production of $T_{5/3}$ with $T_{5/3}$ decays to tW with a 100% branching fraction.

It is assumed that $T_{5/3}$ is heavier than the B quark. The analysis is based on searching for same-sign leptons, from the two W bosons from one of the $T_{5/3}$. Requiring same-sign leptons eliminates most of the standard model background processes, leaving those with smaller cross sections: $t\bar{t}$, W, $t\bar{t}Z$, WWW, and same-sign WW. In addition backgrounds from instrumental effects due to charge misidentification are considered. The CMS search also utilizes jet substructure techniques to identify boosted $T_{5/3}$ topologies. These searches restrict the $T_{5/3}$ mass to be higher than 770 GeV [84].

The single $T_{5/3}$ production cross section depends on the coupling constant λ of the $tWT_{5/3}$ vertex. ATLAS has performed an analysis of same-sign dileptons for the cases where $\lambda = 1$, $\lambda = 3$ which includes both the single and pair production, and for $\lambda \ll 1$, which corresponds to pair production only. This analysis leads to a 95% C.L. lower limit on the mass of the $T_{5/3}$ of 680, 700, and 670 GeV for $\lambda = 1, 3$ and $\ll 1$, respectively.

2.5 Colorons, Z' and Colored Scalars

These particles are associated with top-condensate and top-seesaw models, which involve an enlarged color gauge group. The new particles decay to dijets, $t\bar{t}$, and $b\bar{b}$.

Direct searches for colorons, W', Z', color-octect scalars and other heavy objects decaying to $q\overline{q}$, qg, qq, or gg has been performed using LHC data from pp collisions at $\sqrt{s}$ =7 and 8 TeV. Based on the analysis of dijet events from a data sample corresponding to a luminosity of 19.6 fb^{-1}, the CMS experiment excludes pair production of colorons with mass between $1.20 - 3.60$ and $3.90 - 4.08$ TeV at 95% C.L., color-octet scalars (s8) with masses between $1.20 - 2.79$ TeV, W' bosons with masses below 2.29 TeV, and Z' Boson with masses below 1.68 TeV, as shown in Fig. 5 [85].

A search for pair-produced colorons based on an integrated luminosity of 5.0 fb^{-1} at $\sqrt{s} = 7$ TeV by CMS excludes colorons with masses between 250 GeV and 740 GeV, assuming colorons decay 100% into $q\overline{q}$ [87]. This analysis is based on events with at least four jets and two dijet combinations with similar dijet mass.

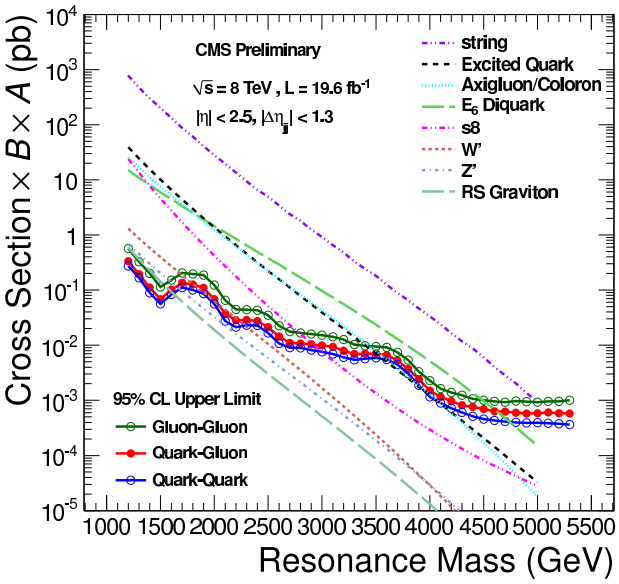

Figure 5: Observed 95% C.L. limits on $\sigma \times B \times A$ for string resonances, excited quarks, axigluons, colorons, E6 diquarks, s8 resonances, W' and Z' bosons, and Randall-Sundrum gravitons [85].

3. Conclusions

As the above analyses have demonstrated, there is already substantial sensitivity to possible new particles predicted to accompany the H in dynamical frameworks of electroweak symmetry breaking. No hints of any deviations from the standard model have been observed, and limits typically at the scale of a few hundred GeV to 1 TeV are set.

Given the need to better understand the H and to pin down how it behaves, we expect that such analyses will be a major theme of the next run of the LHC, and we look forward to increased sensitivity as a result of the higher luminosity and increased centre of mass energy of collisions.

References

1. G. Aad *et al.* [ATLAS Collab.], Phys. Lett. B **716**, 1 (2012) [arXiv:1207.7214 [hep-ex]].
2. S. Chatrchyan *et al.* [CMS Collab.], Phys. Lett. B **716**, 30 (2012) [arXiv:1207.7235 [hep-ex]].
3. S. Weinberg, Physica A **96**, 327 (1979).

4. A. Manohar and H. Georgi, Nucl. Phys. B **234**, 189 (1984).
5. H. Georgi, Nucl. Phys. B **266**, 274 (1986).
6. R. S. Chivukula, hep-ph/0011264.
7. R. S. Chivukula, M. J. Dugan and M. Golden, Phys. Rev. D **47**, 2930 (1993) [hep-ph/9206222].
8. S. Weinberg, Phys. Rev. D **13**, 974 (1976).
9. S. Weinberg, Phys. Rev. D **19**, 1277 (1979).
10. L. Susskind, Phys. Rev. D **20**, 2619 (1979).
11. K. Lane, hep-ph/0202255.
12. C. T. Hill and E. H. Simmons, Phys. Rept. **381**, 235 (2003), [Erratum-*ibid.,* **390**, 553 (2004)] [hep-ph/0203079.
13. R. Shrock, hep-ph/0703050 [HEP-PH].
14. E. Eichten *et al.*, Rev. Mod. Phys. **56**, 579 (1984) [Addendum-*ibid.,* **58**, 1065 (1986)].
15. E. Eichten *et al.*, Phys. Rev. D **34**, 1547 (1986).
16. R. S. Chivukula and V. Koulovassilopoulos, Phys. Lett. B **309**, 371 (1993) [hep-ph/9304293].
17. B. Holdom, Phys. Lett. B **150**, 301 (1985).
18. K. Yamawaki, M. Bando, and K. -i. Matumoto, Phys. Rev. Lett. **56**, 1335 (1986).
19. T. W. Appelquist, D. Karabali, and L. C. R. Wijewardhana, Phys. Rev. Lett. **57**, 957 (1986).
20. T. Appelquist and L. C. R. Wijewardhana, Phys. Rev. D **35**, 774 (1987).
21. T. Appelquist and L. C. R. Wijewardhana, Phys. Rev. D **36**, 568 (1987).
22. E. Gildener and S. Weinberg, Phys. Rev. D **13**, 3333 (1976).
23. Z. Chacko, R. Franceschini, and R. K. Mishra, JHEP **1304**, 015 (2013) [arXiv:1209.3259 [hep-ph]].
24. B. Bellazzini *et al.*, Eur. Phys. J. C **73**, 2333 (2013) [arXiv:1209.3299 [hep-ph]].
25. B. Bellazzini *et al.*, arXiv:1305.3919 [hep-th].
26. Z. Chacko, R. K. Mishra, and D. Stolarski, arXiv:1304.1795 [hep-ph].
27. J. R. Ellis, M. K. Gaillard, and D. V. Nanopoulos, Nucl. Phys. B **106**, 292 (1976).
28. M. A. Shifman *et al.*, Sov. J. Nucl. Phys. **30**, 711 (1979) [Yad. Fiz. **30**, 1368 (1979)].
29. A. I. Vainshtein, V. I. Zakharov, and M. A. Shifman, Sov. Phys. Usp. **23**, 429 (1980) [Usp. Fiz. Nauk **131**, 537 (1980)].

30. S. R. Coleman and J. Mandula, Phys. Rev. **159**, 1251 (1967).
31. M. Bando, K. -i. Matumoto, and K. Yamawaki, Phys. Lett. B **178**, 308 (1986).
32. W. D. Goldberger, B. Grinstein, and W. Skiba, Phys. Rev. Lett. **100**, 111802 (2008) [arXiv:0708.1463 [hep-ph]].
33. E. Eichten, K. Lane, and A. Martin, arXiv:1210.5462 [hep-ph].
34. D. B. Kaplan and H. Georgi, Phys. Lett. B **136**, 183 (1984).
35. D. B. Kaplan, H. Georgi, and S. Dimopoulos, Phys. Lett. B **136**, 187 (1984).
36. K. Agashe, R. Contino, and A. Pomarol, Nucl. Phys. B **719**, 165 (2005).
37. G. F. Giudice *et al.*, JHEP **0706**, 045 (2007) [hep-ph/0703164].
38. M. E. Peskin, Nucl. Phys. B **175**, 197 (1980).
39. R. Barbieri and A. Strumia, hep-ph/0007265.
40. N. Arkani-Hamed, A. G. Cohen, and H. Georgi, Phys. Lett. B **513**, 232 (2001) [hep-ph/0105239].
41. N. Arkani-Hamed *et al.*, JHEP **0208**, 020 (2002) [hep-ph/0202089].
42. N. Arkani-Hamed *et al.*, JHEP **0207**, 034 (2002) [hep-ph/0206021].
43. M. Schmaltz and D. Tucker-Smith, Ann. Rev. Nucl. Part. Sci. **55**, 229 (2005) [hep-ph/0502182].
44. K. Agashe *et al.*, Phys. Lett. B **641**, 62 (2006) [hep-ph/0605341].
45. R. S. Chivukula, A. G. Cohen, and K. D. Lane, Nucl. Phys. B **343**, 554 (1990).
46. W. A. Bardeen, C. T. Hill, and M. Lindner, Phys. Rev. D **41**, 1647 (1990).
47. C. T. Hill, Phys. Lett. B **266**, 419 (1991).
48. B. A. Dobrescu and C. T. Hill, Phys. Rev. Lett. **81**, 2634 (1998) [hep-ph/9712319].
49. R. S. Chivukula *et al.*, Phys. Rev. D **59**, 075003 (1999) [hep-ph/9809470].
50. S. Dimopoulos and L. Susskind, Nucl. Phys. B **155**, 237 (1979).
51. E. Eichten and K. D. Lane, Phys. Lett. B **90**, 125 (1980).
52. D. B. Kaplan, Nucl. Phys. B **365**, 259 (1991).

53. R. S. Chivukula, B. A. Dobrescu, and E. H. Simmons, Phys. Lett. B **401**, 74 (1997) [hep-ph/9702416].
54. R. S. Chivukula and H. Georgi, Phys. Lett. B **188**, 99 (1987).
55. G. D'Ambrosio *et al.*, Nucl. Phys. B **645**, 155 (2002) [hep-ph/0207036].
56. K. Agashe *et al.*, hep-ph/0509117.
57. Y. Grossman and M. Neubert, Phys. Lett. B **474**, 361 (2000).
58. T. Gherghetta and A. Pomarol, Nucl. Phys. B **586**, 141 (2000).
59. T. Appelquist and R. Shrock, Phys. Lett. B **548**, 204 (2002) [hep-ph/0204141].
60. B. Keren-Zur *et al.*, Nucl. Phys. B **867**, 429 (2013) [arXiv:1205.5803 [hep-ph]].
61. J. M. Maldacena, Adv. Theor. Math. Phys. **2**, 231 (1998) [hep-th/9711200].
62. For a review, see C. Csaki, J. Hubisz, and P. Meade, hep-ph/0510275;
    See also J. Parsons, A. Pomarol, *'Extra Dimensions'* review, section *III.2*, in this volume.
63. E. T. Neil, PoS LATTICE **2011**, 009 (2011) [arXiv:1205.4706 [hep-lat]].
64. J. Giedt, PoS LATTICE **2012**, 006 (2012).
65. T. Appelquist *et al.*, arXiv:1309.1206 [hep-lat].
66. R. S. Chivukula, S. B. Selipsky, and E. H. Simmons, Phys. Rev. Lett. **69**, 575 (1992) [hep-ph/9204214].
67. F. del Aguila *et al.*, Nucl. Phys. B **334**, 1 (1990).
68. S. Chatrchyan *et al.*, [CMS Collab.], Phys. Rev. Lett. **107**, 271802 (2011) [arXiv:1109.4985 [hep-ex]].
69. CMS-PAS-B2G-12-021, CERN, Geneva (2013).
70. S. Chatrchyan *et al.*, [CMS Collab.], accepted by PRL (2013) [arXiv:1309.2030 [hep-ex]].
71. S. Chatrchyan *et al.*, [CMS Collab.], Phys. Lett. **B718**, 307 (2012) arXiv:1209.0471 [hep-ex].
72. S. Chatrchyan *et al.*, [CMS Collab.], Phys. Rev. **D86**, 112003 (2012) arXiv:1209.1062 [hep-ex].
73. ATLAS-CONF-2013-051, CERN, Geneva (2013).
74. ATLAS-CONF-2013-017, CERN, Geneva (2013).
75. CMS-PAS-EXO-12-061, CERN, Geneva (2012).
76. ATLAS-CONF-2013-066, CERN, Geneva (2013).

77. ATLAS-CONF-2013-052, CERN, Geneva (2013).
78. ATLAS-CONF-2013-060, CERN, Geneva (2013).
79. ATLAS-CONF-2013-056, CERN, Geneva (2013).
80. CMS-PAS-B2G-12-015, CERN, Geneva (2013).
81. CMS-PAS-B2G-12-019, CERN, Geneva (2013).
82. R. Contino and G. Servant, JHEP **0806**, 026 (2008) arXiv:0801.1679 [hep-ex].
83. J. Mrazek and A. Wulzer, Phys. Rev. **D81**, 075006 (2010) arXiv:0909.3977 [hep-ph].
84. CMS-PAS-B2G-12-012, CERN, Geneva (2013).
85. CMS-PAS-EXO-12-059, CERN, Geneva (2013).
86. ATLAS-CONF-2013-074, CERN, Geneva (2013).
87. S. Chatrchyan *et al.*, [CMS Collab.], Phys. Rev. Lett. **110**, 141802 (2013).
88. ATLAS-CONF-2013-015, CERN, Geneva (2013).
89. CMS-PAS-EXO-12-025, CERN, Geneva (2013).
90. CMS-PAS-EXO-12-024, CERN, Geneva (2013).
91. CMS-PAS-EXO-12-025, CERN, Geneva (2013).
92. CMS-PAS-B2G-12-010, CERN, Geneva (2013).
93. ATLAS-CONF-2013-050, CERN, Geneva (2013).
94. CMS-PAS-EXO-12-023, CERN, Geneva (2013).